

# Numerical Modelling of Dynamic Earth Force Transmission to Underground Structures

**N. Kodama**

*Waseda Institute for Advanced Study, Waseda University, Japan*

**K. Komiya**

*Chiba Institute of Technology, Japan*



## SUMMARY:

The forces applied to a structure from the soil ground during an earthquake and the dynamic response of a structure are problems that are not well understood. In recent years, seismic design technology aided by numerical simulation is under active development. Successful improvement of the accuracy and reliability of numerically simulated results relies on a clear understanding of the seismic force transmission mechanism between the soil and a structure associated with mechanical properties of soil.

In this study, laboratory shaking tests are conducted to know the dynamic earth pressure-displacement behaviours in the interface between soft soils and a structure. The test apparatus are designed to have a structure move only by its inertial force and the lateral earth pressure that comes from surrounding soils. In the tests, the earth pressure on the structure surface and the relative displacement between the soil and the structure are measured under various conditions.

A new simple finite element, which models the dynamic interface behaviour between the soft soil and the structure is proposed from the experimental results. Estimated seismic responses of a bridge pier calculated by the proposed interface model, conventional linear elastic model and tension cut-off model are compared.

*Keywords: Soil-structure dynamic interaction, Laboratory shaking test, Finite element method*

## 1. INTRODUCTION

The basic concept of seismic designs and technologies is to ensure that structures resist the largest earthquake on record without collapse [e.g. AASHTO (2007), JRA (2002)]. The forces applied to a structure from the soil ground during an earthquake and the dynamic response of a structure against seismic motions are problems that are not well understood and highly structured. Safety factors are widely used in the design to compensate the uncertainty associated with these problems. In recent years, seismic design technology aided by numerical analyses is under active development. The improvement of the accuracy and reliability of numerical simulations can not be achieved without a clear understanding of the seismic force transmission mechanism between the soil and a structure.

In a seismic force transmission mechanism problem, the main concerns are the earth pressure applied at the interface of the structure and the soil, the displacement of the structure and the deformation of the soil. A soil-spring is the most commonly used numerical model to apply seismic forces and traction to a structure and to impose displacement boundary conditions [e.g. AASHTO (2007), JRA (2002)]. However, the soil-spring stiffness is generally determined without regard to the stress-strain behaviour of the soil, which depends on its stress history and its properties such as water content, bulk density and grain size distribution.

The authors have provided that some model test results of the dynamic behaviour between soft soils and an underground structure, and indicated that an elasto-viscoplastic model with Mohr-Coulomb yield criteria is adequate for simulations of the relationship [e.g. Kodama et al. (2009), Kodama and Komiya (2010)]. However that nonlinear dynamic soil-structure analysis was unable to match with complex situations in the field since it involved a series of complex procedures and stages e.g. predictions of dynamic plastic parameters, of actual stress histories et.al.

In this study, a new finite element modelled the dynamic earth pressure-displacement behaviour of an interface between the soil and the structure is proposed from laboratory shaking tests results. Two dimensional finite element analyses of dynamic response of a bridge pier during earthquake are carried out in which the proposed interface element is used to estimate the soil-foundation dynamic interaction. The simulated results are compared with those of a numerical model using the conventional linear elastic and tension cut-off interface models.

## 2. MODEL SHAKING TESTS

### 2.1. Outline of Laboratory Shaking Test

Laboratory shaking tests are carried out to investigate a dynamic interaction between soil and a structure. A schematic diagram of the laboratory shaking test apparatus is shown in Fig. 2.1 [Kodama and Komiya (2010)]. The shaking of the tank is allowed in only one horizontal direction as shown in Fig. 2.1.

Inside of the shaking tank, a hollow rectangular structure model made of steel with 40 cm width, 30 cm depth and 80 cm height is placed in its centre. The mass of the structure model is set to 50, 75, 100 or 150 kg. At the both sides of the structure model, rectangular parallelepiped model grounds of 40 cm width, 30 cm depth and 40 or 60 cm height are made as shown in Fig. 2.1. On the boundary between the bottom face of the structure model and the inner surface of the tank, ball bearings are made of steel are installed to cut off the lateral force travelled through the boundary [Komiya et al. (2006)]. The soil grounds are made by tamping to fill the gaps between the structure model and the tank. When the tank is shaking, therefore, only the lateral forces coming from the soil grounds act upon the structure model except for bearing vertical support forces.

The earth force applying to the structure model is measured by pressure transducers installed on the structure model as shown in Figure Fig. 2.1. The relative displacement between the structure model and the tank is measured by a laser distance sensor attached to the tank.

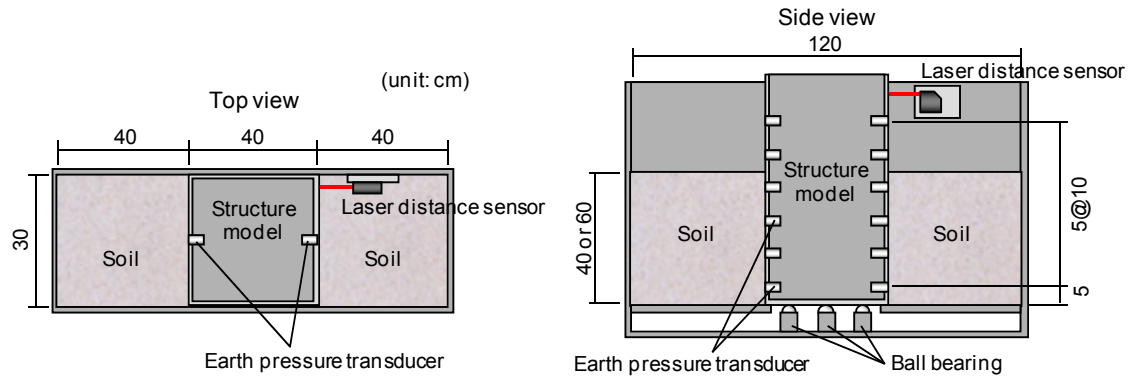


**Figure 2.1.** Shaking tank details [Kodama and Komiya (2010)]

**Table 2.1.** Soil test results

Density $\rho$ (g/cm <sup>3</sup> )		2.658
Element contents	Clay (%)	12.29
	Silt (%)	7.50
	Fine sand (%)	77.02
	Medium sand (%)	3.19
Uniformity coefficient $U_c$		56.70
Curvature coefficient $U'_c$		28.40
Mean grain size $D_{50}$ (mm)		0.16
Optimum water content $w_{opt}$ (%)		10.64
Maximum dry density $\rho_{max}$ (g/cm <sup>3</sup> )		1.804

**Table 2.2.** Shaking test parameters

Soil property	Initial mass density $\rho_0$ (g/cm <sup>3</sup> )	1.91
	Initial void ratio $e_0$	0.54
	Water content $w$ (%)	10.6
	Soil depth $d$ (cm)	40
Structure property	Mass (kg)	120
Sinusoidal shaking waveform	Frequency (Hz)	4
	Displacement amplitude (mm)	10
	Maximum acceleration (gal)	632

Soil ground used in the test is made of Toyoura Sand and Kaoline-clay. The soil parameters and the shaking test parameters are shown in Table 2.1 and Table 2.2, respectively.

## 2.2. Laboratory Shaking Test Results

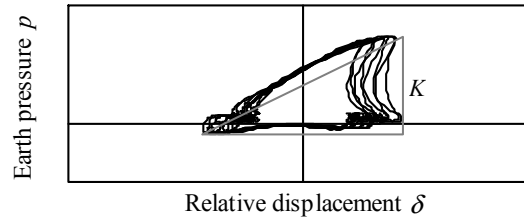
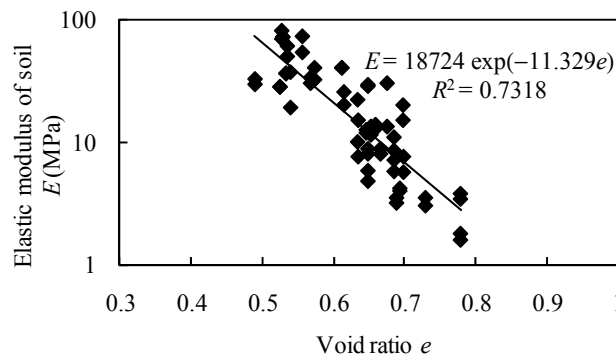
Experimental earth pressure-relative displacement relations on the structure wall are measured at the depth of 5 cm lower from the soil surface and further every 10 cm. Elastic modulus of soil  $E$  is calculated by assuming one-dimensional compression from the gradient of the earth pressure-relative displacement relation curve under compressive loading  $K$  (Eqn. 2.1).

$$E = KW \quad (2.1)$$

where  $W$  is a compression span that is 40 cm in this experiment. Gradient  $K$  is calculated as follows:

$$K = (p_{max} - p_{min}) / (\delta_{max} - \delta_{min}) \quad (2.2)$$

where  $p_{max}$  and  $p_{min}$  are the maximum and the minimum earth pressure,  $\delta_{max}$  and  $\delta_{min}$  are the maximum and the minimum relative displacement after the curve has reached a stationary state (Fig. 2.2).

**Figure 2.2.** Typical example of gradient  $K$  calculation**Figure 2.3.** Typical example of gradient  $K$  calculation

Elastic modulus of the soil at the depth of 5 cm upper from the bottom of the tank  $E_{bottom}$  is approximated by the void ratio of soil  $e$  by Eqn. 2.3, that is obtained by least square fitting from the results of 31 shaking tests as shown in Fig. 2.3.

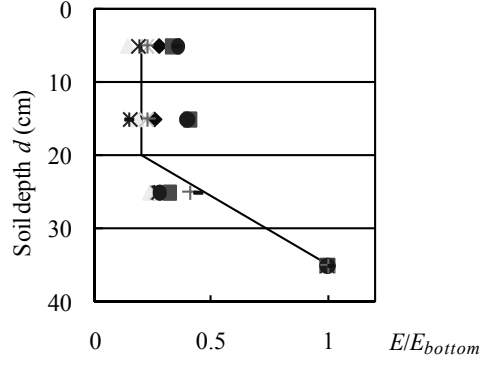


**Figure 2.4.** Typical example of gradient  $K$  calculation

$$E_{bottom} = 18700 \exp(-11.3 e) \quad (2.3)$$

Elastic modulus of soil  $E$  also varies according to the soil depth. Fig. 2.4 shows the variation of normalised elastic modulus  $E$  with respect to  $E_{bottom}$ . The static lateral earth pressure increases with increasing soil depth [e.g. Lambe and Whitman (1969)]. This property was also observed in the dynamic lateral earth pressure measured in our experiments, which was implied in the distribution of the fraction  $E/E_{bottom}$  shown in Fig. 2.4. We discuss here only the experimental results of the deepest earth pressure observation point, because in shallow soil, the magnitude of the dynamic lateral earth pressure is relatively small and furthermore soil particles can easily change its position under low vertical pressure, and that makes difficult to observe the earth pressure accurately. Relation between the soil depth  $d$  (cm) and the fraction  $E/E_{bottom}$  is simply modelled by following equations to determine the elastic modulus distribution in depth.

$$E/E_{bottom} = \begin{cases} 0.2 & (d < 20) \\ 0.2 + 4(d - 20) / 75 & (d \geq 20) \end{cases} \quad (2.4)$$

### 3. STRESS-STRAIN RELATION MODELLING OF SOIL-STRUCTURE INTERFACE

From a study of the results of the experiment described in the previous section, a new model for soil that represents the normal stress-strain relations perpendicular to the wall of the structure is proposed here. The stress-strain diagram shown in Fig. 3.1(a) shows the features of the proposed model. In this model, normal elastic modulus  $E_n$  is a function of normal strain increment  $d\epsilon_n$ . When  $d\epsilon_n$  is positive (compressive increment here),  $E_n$  equals to the elastic modulus of the soil  $E$  (paths OA and CD), and when  $d\epsilon_n$  is negative (tensile increment here),  $E_n$  equals to zero and the normal stress  $\sigma_n$  immediately turns to zero (paths ABC and DEO).

There is a clear difference in modelling of the unloading path between the proposed model and a tension cut-off model (Figure Fig. 3.1(b)). In the unloading paths, the normal elastic modulus  $E_n$  of the

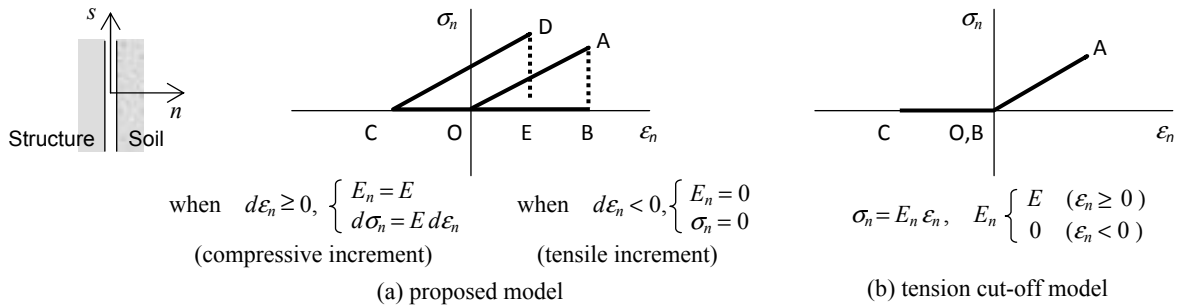


**Figure 3.1.** Stress-strain models of the soil-structure interface

proposed model is always set to zero, while that of the tension cut-off model keeps the initial elastic modulus  $E$  until the normal strain  $\varepsilon_n$  decreases to zero (paths ABC in Figure Fig. 3.1(b)).

#### 4. NUMERICAL SIMULATION RESULTS

A case of the model shaking test is simulated by direct time integration method. Finite Element model for the simulation is shown in Fig. 4.1. The soil and the structure model were modelled by 8-nodes plane strain elements [Washizu et al. (1994)], and the interface between soil elements and structure elements was modelled by 6-nodes quadrilateral anisotropic elements [Smith and Griffiths (2004)]. Sinusoidal displacement boundary condition was applied to nodes highlighted by circles in Fig. 4.1.

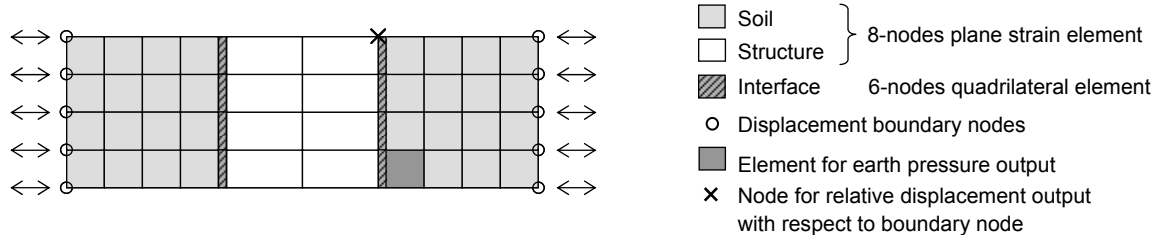


**Figure 4.1.** Finite Element model for simulation

Three different models of the normal stress-strain relations perpendicular to the wall of the structure, or local  $\xi$ -direction of an interface element were examined. Fig. 4.2(a) shows the normal stress-strain relation of the proposed model in this paper. In this model, normal elastic modulus  $E_\xi$  is a function of normal strain increment  $d\varepsilon_\xi$ . When  $d\varepsilon_\xi$  is positive (compressive increment here),  $E_\xi$  equals to the elastic modulus of the soil  $E$ , and when  $d\varepsilon_\xi$  is negative (tensile increment here),  $E_\xi$  equals to zero and the normal stress  $\sigma_\xi$  immediately turns to zero. Fig. 4.2(b) shows the linear elastic model in which the normal stress  $\sigma_\xi$  is always calculated as the product of the elastic modulus  $E$  and the normal strain  $\varepsilon_\xi$ . Fig. 4.2(c) shows the tension cut-off model in which also  $\sigma_\xi$  is proportional to  $\varepsilon_\xi$ , but the proportionality factor changes from  $E$  to zero when  $\varepsilon_\xi$  is negative.

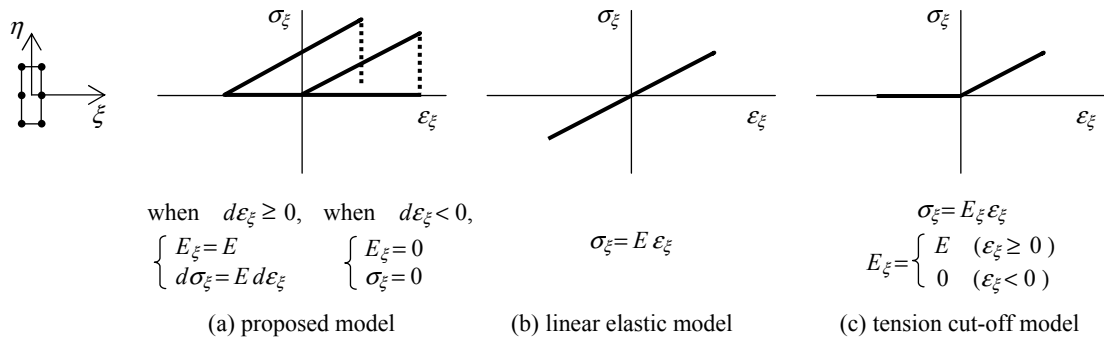


**Figure 4.2.** Stress-strain models for interface element

**Table 4.1.** Material parameters for numerical analyses

Parameter		Soil	Interface	Structure
Elastic modulus $E$ (MPa)	depth = 5 cm	8.37		2.1E+5
	depth = 15 cm	8.37		
	depth = 25 cm	19.53		
	depth = 35 cm	41.86		
Poisson's ratio $\nu$		0.31	—	0.3
Mass density $\rho$ (g/cm3)		1.91	—	2.5
Mass proportional damping coefficient $\alpha$		1.0	—	1.0

Material parameters used in the simulation are shown in Table 4.1. Elastic moduli of soil and interface were calculated from Eqns. 2.3 and 2.4 using the initial void ratio  $e_0$  shown in Table 2.2. Mass proportional damping coefficient of Rayleigh damping  $\alpha$  was introduced to avoid excess oscillation, which is remarkable when the linear elastic model or the tension cut-off model are used. The damping factor  $\alpha = 3.3$  is calculated assuming that the first and the third modal damping factors of the system  $h_1$  and  $h_3$  are both 0.01. These two modes are predominant in horizontal oscillation, and those natural frequencies are  $f_1 = 40.5\text{Hz}$  and  $f_3 = 78.7\text{Hz}$  respectively.

Fig. 4.3 shows experimental and numerically simulated earth pressure-relative displacement relations. Three types of interface stress-strain model, including the proposed model, the linear elastic model and the tension cut-off model, were used in the simulations. The proposed model gives a good approximation to the experimental hysteresis curve (Fig. 4.3(a)). Fig. 4.4 and Fig. 4.5 show the time histories of relative displacement and earth pressure at 35 cm depth respectively. As shown in Fig. 4.4, all the models can give good approximations to the maximum value of the relative displacement, but the time histories estimated by the linear elastic and the tension cut-off interface models seem to be dominated by higher frequency components than the experimental result.

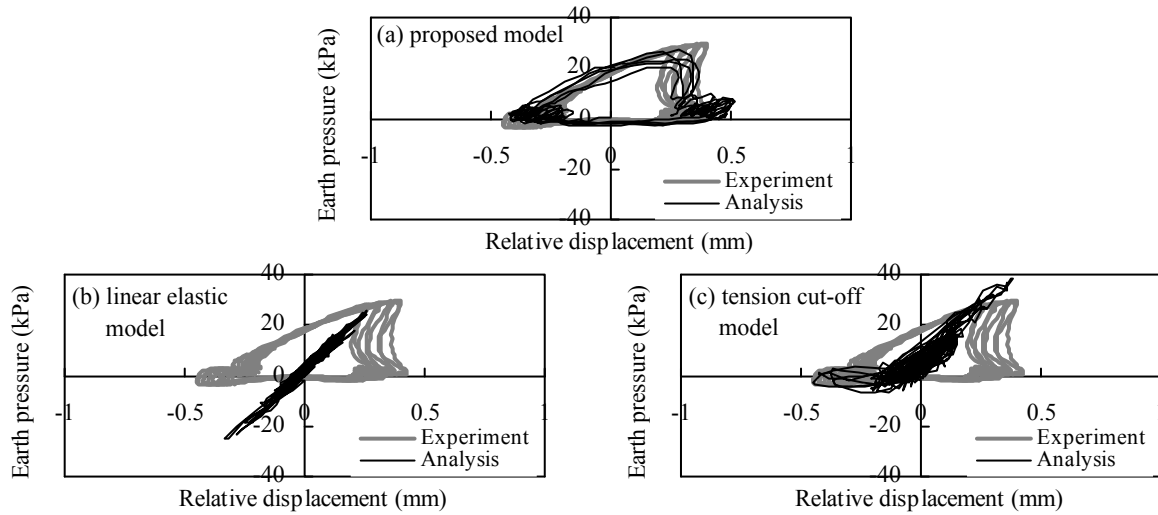


**Figure 4.3.** Comparison of experimental and analytical earth pressure-relative displacement relations at 35 cm depth

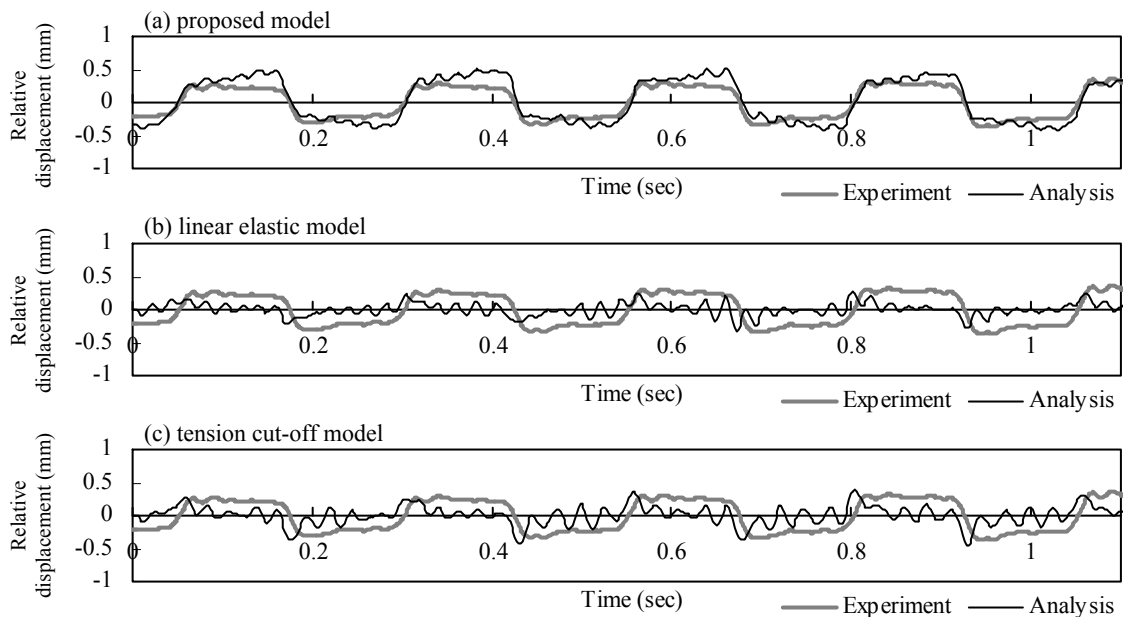


**Figure 4.4.** Comparison of experimental and analytical relative displacement time histories

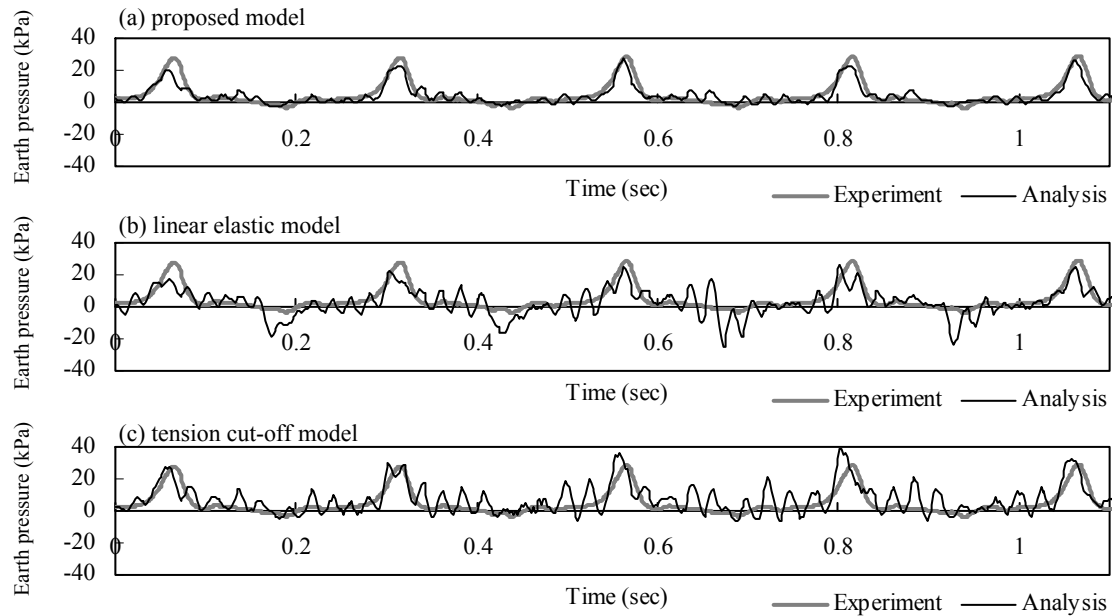


**Figure 4.5.** Comparison of experimental and analytical earth pressure time histories at 35 cm depth

The time histories of the experimental and the numerically estimated earth pressure are compared in Fig. 4.5. It indicates that the result estimated by the proposed model shows good agreement with the experimental result. Fig. 4.5(b) indicates that the linear elastic interface model estimates that noticeable negative stress (tensile stress here) can be applied to the structure, which was observed at a low level in the experiments.

## 5. APPLICATION TO DYNAMIC RESPONSE ANALYSIS OF PIER

In order to examine the influence of interface stress-strain modelling to numerical simulations, the dynamic response in the bridge transverse direction of a simple pier of a simply supported girder bridge shown in Fig. 5.1 to a seismic motion is calculated using the proposed, the linear elastic and the tension cut-off interface models. In bridge seismic design, the stresses and deformations of the bridge members are checked in two orthogonal directions, except when a bridge pier is located on the edge of an embankment where the earth pressure varies largely with direction, which are generally bridge transverse and longitudinal axes [e.g. AASHTO (2007), JRA (2002)]. It is supposed that the pier oscillation can be calculated independently of other parts of the bridge because movable bearings are installed on the top of the pier. Fig. 5.2 shows the acceleration record observed at 1995 Kobe Earthquake used as input waveform. The maximum acceleration is 812 gals and the predominant frequency is around 1.4 Hz.

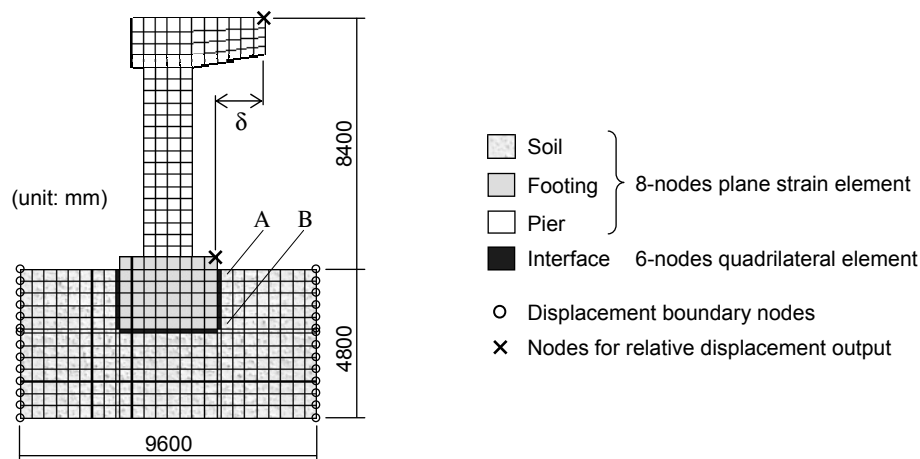


**Figure 5.1.** Simple pier model for dynamic response analysis

Fig. 5.3 shows the lateral stress distribution calculated by three different interface stress-strain models. Time histories of the lateral stress of a soil element located at the ground surface of the right side of the footing are shown in Fig. 5.4. The proposed model gives lower peak values of stresses compared to the linear elastic and the tension cut-off model. The differences of the calculated results predicted by different interface models are more clearly recognised by comparing earth pressure-relative displacement relations shown in Fig. 5.5. The positions of elements A and B are represented in Fig. 5.1. Even though the proposed model does not allow for dumping effects in the material properties, the time delay is represented in the output of the earth pressure-relative displacement relations. Time histories and Fourier amplitude spectra of the relative displacement  $\delta$  are shown in Fig. 5.6. The proposed model estimates the predominant frequency of the response of the system to the applied acceleration even lower than the tension cut-off model and the linear elastic model. These results show that different stress-strain models of an interface element can cause different evaluation of the system response both in time domain and frequency domain. It indicates that proper modelling of the soil-structure interaction is important in predicting the maximum displacement and predominant response frequencies of the system.

## 6. CONCLUSIONS

In this paper, a new dynamic earth force transmission model for a sandy soil-structure interface was proposed based on experimental results of laboratory shaking tests.

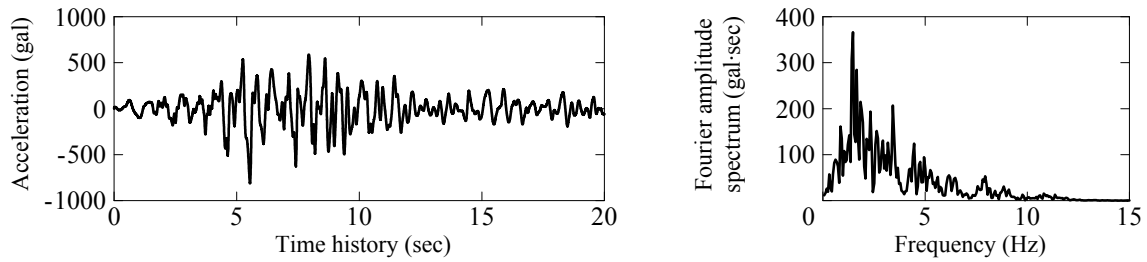


**Figure 5.2.** Time history and Fourier amplitude spectrum of acceleration record for input waveform

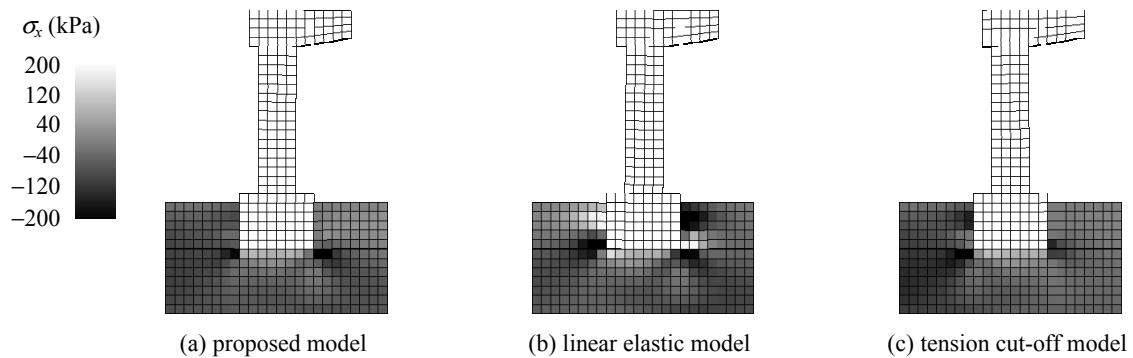


**Figure 5.3.** Distribution of horizontal stress  $\sigma_x$  in soil at 7.9 seconds of analyses

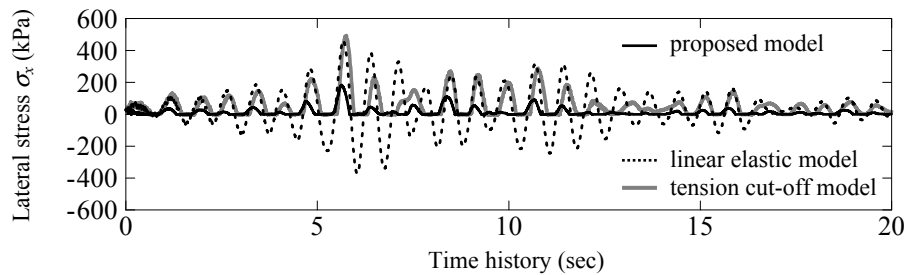


**Figure 5.4.** Comparison of time histories of lateral stress of the soil element beside the footing at the ground surface (Element A shown in Fig. 5.1)



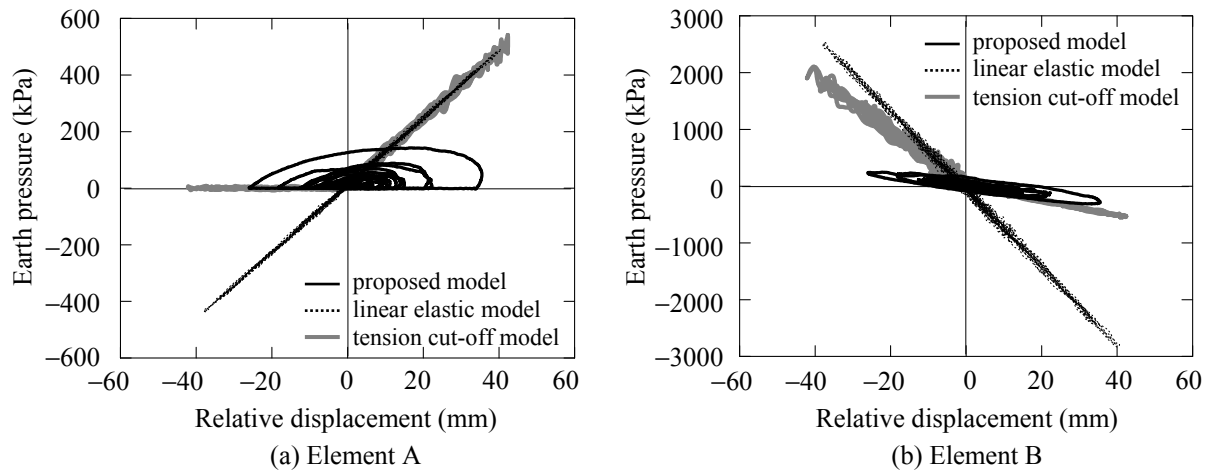


**Figure 5.5.** Comparison of earth pressure-relative displacement relations predicted by different interface models

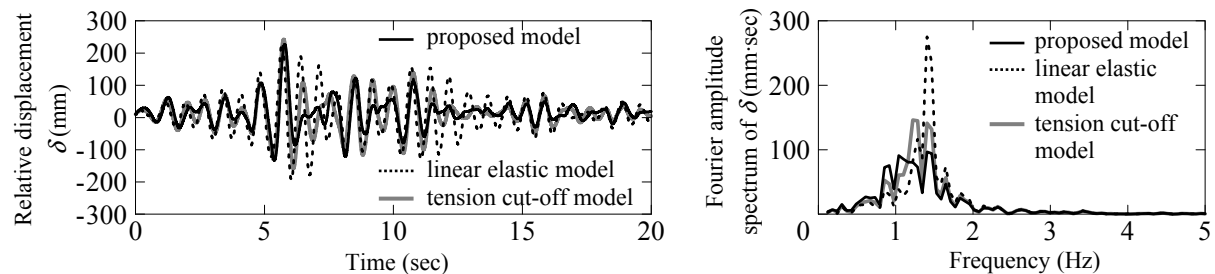


**Figure 5.6.** Comparison of time histories and Fourier amplitude spectra of relative displacement  $\delta$

The proposed model gave good approximations to the earth pressure-relative displacement hysteresis curve, as well as the time histories of relative displacement and earth pressure. The effectiveness of the proposed model was shown in comparison of the simulated results of the laboratory shaking tests by different mechanical models of the soil-structure interface, namely conventional linear elastic model and the tension cut-off model.

Two dimensional finite element analyses of the dynamic responses of a bridge pier against seismic force were carried out. The proposed interface model gave different estimations of the system response both in time domain and frequency domain compared to the results calculated by tension cut-off interface model. It indicates that to predict dynamic response of a structure against seismic earth force, it is important to use proper soil-structure interaction model.

## REFERENCES

- American Association of State Highway and Transportation Officials (2007). AASHTO LRFD Bridge Design Specifications - SI Units (4th Edition).
- Japan Road Association (2002). Design Specification for Highway Bridges, Part V Seismic Design.
- Kodama, N. and Komiya, K. (2010). Model experiment and numerical modelling of dynamic soil-structure interaction. *Materials with Complex Behaviour, Advanced Structured Materials* **3**, 269-278.
- Kodama N., Komiya K. and Morozumi T. (2009). Numerical simulation of soil-tunnel dynamic interaction. *2nd International Conference on Computational Methods in Tunnelling*. 71-76.
- Komiya, K., Shikata, K. and Kodama, N. (2006). Aseismic effect of ground improved with acrylic emulsion. *The First European Conference on Earthquake Engineering and Seismology*. Paper number 1657.
- Lambe, T. W. and Whitman, R. V. (1969). Soil mechanics, John Wiley & Sons, New York, U.S.A.
- Smith, I. M. and Griffiths, D. V. (2004). Programming the finite element method, John Wiley & Sons, Chichester, U.K.
- Washizu, K. et al. (1994). Handbook of the Finite Element Method (Basics), Baifukan, Tokyo, Japan (in Japanese).